

and broadening parameters of excitonic bands. We can distinguish, then, two different cases. In the first one, the shift effect is important, as in the case of the Γ_1 exciton; in fact, the Γ_1 exciton, as the crystal goes from room temperature to 90°K, shifts 0.2 eV, with a rate of -9.5×10^{-4} eV/°K. In the second case, only the broadening must be taken into account, as in the case of the exciton E . In effect, the E structure has a dispersionlike line shape and the zero energy crossing is independent of T , while the broadening is strongly dependent. Similar dispersionlike structure has also been observed in room-temperature spectra of KI¹³ [7.4 eV in Fig. 3(a)]. Then, if it is reasonable that the spin-orbit-split excitons both behave in the same way with respect to temperature, the E structure cannot be attributed to the $\Gamma_1 + \Delta$ exciton.^{2,5} On the other hand, it is possible to associate the E exciton with the X_3 edge, in agreement with the calculations of Kunz for KI and RbI crystals. Moreover, Kunz has calculated very small pressure coefficients for the X_3 transitions in KI,⁷ and this could mean that, for KI and also for RbI, the X_3 transitions do not change their energy with temperature, assuming of course that the energy shift depends on temperature only through the change in lattice parameter.⁶

Beyond the E exciton other peaks associated with higher transitions are observed.

Experiments at lower temperatures to obtain a more detailed description of the optical properties of these crystals are in progress.

¹M. Cardona, *Modulation Spectroscopy* (Academic, New York, 1969).

²G. Baldini and B. Bosacchi, *Phys. Rev.* **166**, 863 (1968).

³K. J. Teegarden and G. Baldini, *Phys. Rev.* **155**, 896 (1967).

⁴R. S. Knox and N. Inchauspé, *Phys. Rev.* **116**, 1043 (1959).

⁵Y. Onodera, M. Okazaki, and T. Inui, *J. Phys. Soc. Jap.* **21**, 2229 (1966).

⁶A. B. Kunz, *Phys. Rev.* **151**, 620 (1966).

⁷A. B. Kunz, *J. Phys. Chem. Solids* **31**, 265 (1969).

⁸A. B. Kunz, *Phys. Rev. B* **4**, 1374 (1971).

⁹S. Antoci, E. Reguzzoni, and G. Samoggia, *Phys. Rev. Lett.* **25**, 162 (1970).

¹⁰S. Antoci, E. Reguzzoni, and G. Samoggia, *Solid State Commun.* **9**, 1081 (1971).

¹¹J. W. Hodby, *J. Phys. C: Proc. Phys. Soc., London* **4**, L8 (1971).

¹²G. R. Huggett and K. Teegarden, *Phys. Rev.* **141**, 797 (1966).

¹³Preliminary measurements at 210°K have shown that the energy position of the E structure is temperature independent also in KI.

Charge Localization at Metal-Insulator Transitions in Ti_4O_7 and V_4O_7

M. Marezio, D. B. McWhan, P. D. Dernier, and J. P. Remeika

Bell Laboratories, Murray Hill, New Jersey 07974

(Received 13 April 1972)

Single-crystal x-ray investigations reveal charge localization in the insulating phases of Ti_4O_7 and V_4O_7 . Chains of M^{3+} and M^{4+} sites run parallel to the pseudorutile c axis, whereas the metal valences are disordered in the metallic phases. The $3+$ and some of the $4+$ sites form metal-metal pair bonds, and the unpaired $4+$ sites have one short metal-oxygen distance.

The oxides Ti_4O_7 and V_4O_7 are members of a homologous series of the form $M_n\text{O}_{2n-1}$. Two transitions are observed in the resistivity of Ti_4O_7 at 150 and 125 K.¹ At the 150-K transition there is an accompanying decrease in the magnetic susceptibility,² and a discontinuity in volume.³ There is a single metal-insulator transition in V_4O_7 at 250 K,⁴ and a paramagnetic-antiferromagnetic transition at 40 K.⁵ The 250-K transition is accompanied by changes in resistivity,⁴ magnetic susceptibility,⁶ and volume.³ In this Letter we

present the first crystallographic evidence for charge localization at the metal-insulator transition. This localization is accompanied by either a pairing of adjacent metal atoms or a displacement of the metal atom toward one of the neighboring oxygen atoms. A disordered bond model is suggested for the intermediate phase of Ti_4O_7 . In V_4O_7 the transition is found to be only slightly first order.

Ti_4O_7 and V_4O_7 are isostructural at room temperature⁷ and a detailed structure has been re-

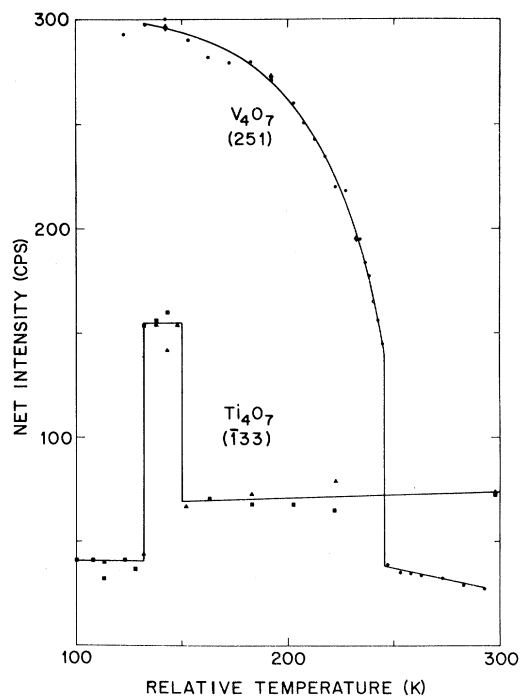


FIG. 1. Net intensity as a function of temperature, showing two distinct first-order transitions in Ti_4O_7 and a single, only slightly first-order transition in V_4O_7 . Diamonds and triangles, data taken while cooling; squares and circles, on warming. The temperature is that of the cooling gas which may be different from that of the crystal.

ported for the former.⁸ The structure consists of a distorted hexagonal close-packed array of oxygens. The cations occupy the octahedral sites so as to form blocks resembling the rutile structure, which are infinite in two dimensions and four octahedra wide in the third. At the crystallo-

graphic shear planes between blocks, there is face sharing between oxygen octahedra containing cations instead of only corner or edge sharing as in rutile. The resulting structure is triclinic with an $A\bar{1}$ space group in which there are 4 and 7 crystallographically independent metal and oxygen atoms, respectively.⁹

The crystal structure of Ti_4O_7 was refined at 298, 140, and 120 K and that of V_4O_7 at 298 and 200 K using the methods described in Ref. 8. The crystals of Ti_4O_7 were those used in the earlier study.⁸ The crystals of V_4O_7 were grown by vapor transport from a powder sample as described by Nagasawa.¹⁰ In the x-ray experiments, the temperature of the crystal was controlled by blowing a stream of nitrogen gas of controlled temperature over it. The transitions are clearly seen in the intensities as illustrated in Fig. 1. The intensity of each reflection was carefully maximized for the different angles on the three-circle diffractometer. After refinement by the least-squares method of the low-temperature structures, the final standard R factors, based on 350 (Ti_4O_7) and 850 (V_4O_7) measured reflections, were always below 3.5%. There was no evidence for a loss of either the A centering or the center of inversion in any of the phases.¹¹ No measurable differences were observed in 20 Friedel pairs of low intensity for each oxide.

The relevant interatomic distances are given in Table I. At the lowest temperatures the size of the cations as measured by the M -O distance is markedly different for different sites, whereas at room temperature the corresponding distances are almost the same in Ti_4O_7 and only slightly different in V_4O_7 . The metal-oxygen distances

TABLE I. Average metal-oxygen distance (\AA) in each octahedra.

Atom	Ti_4O_7				V_4O_7		
	298 K	140 K	120 K	Predicted	298 K	200 K	Predicted
1	2.006(2)	2.011(4)	2.043(4)	2.04 Ti^{3+}	1.967(2)	1.948(2)	1.94 V^{4+}
2	2.006(2)	2.000(4)	1.973(4)	1.98 Ti^{4+}	1.980(2)	1.992(2)	2.01 V^{3+}
3	2.004(2)	2.015(4)	2.044(4)	2.04 Ti^{3+}	1.969(2)	1.961(2)	1.94 V^{4+}
4	2.018(2)	2.012(4)	1.996(4)	1.98 Ti^{4+}	1.984(2)	2.009(2)	2.01 V^{3+}
Metal-Metal Distances (\AA)							
1-3	3.020(1)	2.990(2)	2.802(2)		2.964(1)	3.027(1)	
1-1	2.895(1)	2.926(2)	3.133(2)		2.794(1)	2.687(1)	
2-4	3.019(1)	3.000(2)	3.083(2)		2.930(1)	2.856(1)	
2-2	2.942(1)	2.937(2)	3.023(2)		2.926(1)	3.024(1)	
3-4	2.811(1)	2.806(2)	2.838(2)		2.768(1)	2.781(1)	

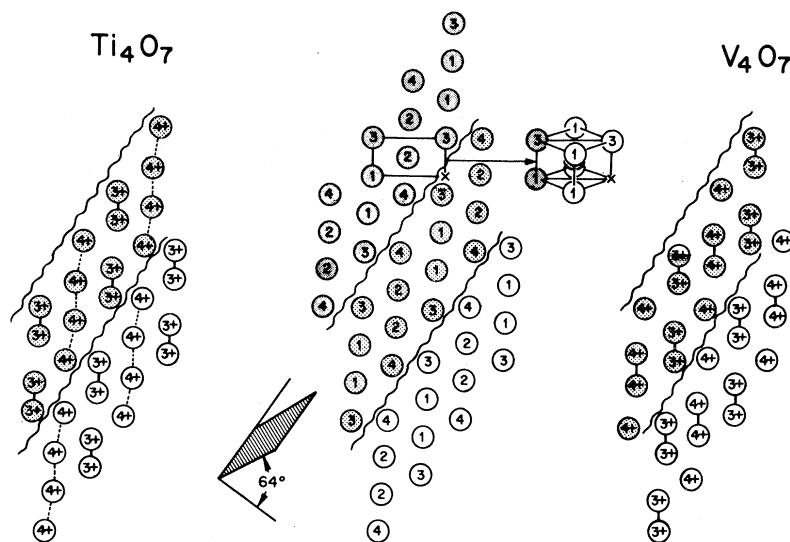


FIG. 2. Diagram showing the pattern of charge localization (+3, +4) and pairing of the cations (heavy lines) in the insulating phases of Ti_4O_7 (left) and V_4O_7 (right). The center figure is the undistorted structure at 298 K. The inset shows the cation positions in rutile and defines the pseudorutile plane shown in the main figures. The numbers in the center figure designate the crystallographically inequivalent sites. The shading and wavy lines show the relation between different rutilelike blocks. There are steps at the shear planes (wavy lines) with each block displaced upward successively on going from the bottom to the top of the figure. In three dimensions the shear planes make an angle of 64° with the plane of the paper as illustrated.

calculated for 3+ and 4+ cations from the ionic radii given by Shannon and Prewitt¹² are in good agreement with the observed values (see Table I).¹³ As shown in Fig. 2, the 3+ or 4+ sites form chains along the pseudorutile c axis, but the chains are interchanged between the Ti and V compounds so that the cations with one d electron are atoms (1) and (3) in both insulating phases. This ordering is contrary to the traditional picture in which the 3+ cations would be at the edge of the rutile block because they have a coordination similar to that observed in Ti_2O_3 .¹⁴ In fact, the $M(3+)-M(4+)$ distance across the shared octahedral face is not anomalously short as in Ti_2O_3 . The crystallographic results clearly show a spontaneous change in the effective size of the cations at the metal-insulator transition which is evidence for charge localization.

In addition to localizing, most of the cations pair at the transition to form short metal-metal bonds. These are listed in Table I and the pattern of pairing illustrated in Fig. 2. The displacements of the anions are a factor of 10 smaller, and only the cations are shown in Fig. 2. The crystallographic data for Ti_4O_7 suggest that the d electrons on adjacent sites pair to form a non-magnetic singlet bond which is compatible with the increase in resistivity and with the decrease in the magnetic susceptibility. A similar model

has been proposed for the metal-insulator transition in pure VO_2 where all, instead of half, the sites have one d electron.¹⁴ In V_4O_7 only two of the four V^{4+} cations are paired, and the magnetic state of the d electrons involved in the V^{3+} pair bonds is not clear. Unpaired V atoms are also found in insulating Cr-doped VO_2 which has strings of paired vanadium atoms alternating with unpaired zigzag chains parallel to the pseudorutile c axis. In all three of these compounds (Ti_4O_7 , V_4O_7 , and $\text{VO}_2 + \text{Cr}$) the unpaired cations are displaced toward one of the oxygen atoms, which leads to one short and one long metal-oxygen distance. Goodenough has suggested that a balance between covalent metal-metal and metal-oxygen bonds causes the distortion at the metal-insulator transition in $\text{VO}_2 + \text{Cr}$, in which the c (rutile) axis doubles.¹⁴ It is not clear how to apply this atomic picture to V_4O_7 .

As shown in Fig. 1 there are two clear transitions in Ti_4O_7 . The decrease in susceptibility and part of the increase in resistivity occurs at 150 K, but the major changes in structure occur at the 125-K transition. In the refinement of the structures the thermal parameters are found to be anomalously large in the intermediate phase. The average root-mean-square thermal displacements \bar{u} for the titanium atoms 1 through 4 are 0.076, 0.074, 0.074, and 0.077 Å at 298 K; 0.078,

0.079, 0.083, and 0.078 Å at 140 K; 0.060, 0.059, and 0.059 Å at 120 K. As \bar{u} is expected to decrease with decreasing temperature, the values for the intermediate phase are substantially larger than those in the phases above and below. In addition, the thermal ellipsoids are highly anisotropic in both low-temperature phases with the major axis along the Ti-Ti bonds. In order to account for the resistivity, susceptibility, and x-ray data in the intermediate phase, it is reasonable to propose that there is charge localization and pairing, but that there is no long-range order in the bonding. The lower transition would then reflect the change from a disordered to an ordered bond state.

In V_4O_7 , with one additional d electron per atom, the nature of the transition is markedly different. The variation in intensity with temperature in Fig. 1 shows that the transition is only weakly first order. As there is no change in symmetry at the transition, it cannot be second order. A similar variation with temperature has been observed in the ^{51}V NMR frequency of the 4+ sites,¹⁵ the resistivity,⁴ and the susceptibility.⁶ This suggests that these properties may be related to the pairing of the cations.

There is a strong analogy between the transitions in Ti_4O_7 and $V_4\text{O}_7$ and that envisioned by Verwey for Fe_3O_4 . In both cases there is disorder in the cation sites above the transition and charge localization below. However, the crystallographic evidence for a change in cationic size is established only for Ti_4O_7 and $V_4\text{O}_7$. More detailed papers on these structures will be published elsewhere.

We are indebted to T. M. Rice for many helpful

discussions. We thank R. F. Bartholomew and W. B. White for kindly supplying the Ti_4O_7 crystals.

¹R. F. Bartholomew and D. R. Frankl, Phys. Rev. **187**, 828 (1969).

²L. N. Mulay and W. J. Danley, J. Appl. Phys. **41**, 877 (1970).

³M. Marezio, P. D. Dernier, D. B. McWhan, and J. P. Remeika, Mater. Res. Bull. **5**, 1015 (1970).

⁴H. Okinaka, K. Nagasawa, K. Kosuge, Y. Bando, S. Kachi, and T. Takada, J. Phys. Soc. Jap. **28**, 798 (1970).

⁵H. Okinaka, K. Kosuge, S. Kachi, M. Takano, and T. Takada, to be published.

⁶K. Nagasawa, Y. Bando, and T. Takada, Jap. J. Appl. Phys. **8**, 1262 (1969).

⁷S. Andersson and L. Jahnberg, Ark. Kemi **21**, 413 (1963).

⁸M. Marezio and P. D. Dernier, J. Solid State Chem. **3**, 340 (1971).

⁹Further work has shown that the refinement based on $P\bar{1}$ in Ref. 8 was a false minimum and that the correct space group is $A\bar{1}$, i.e., the pseudorelation between x, y, z and $x, y + \frac{1}{2}, z + \frac{1}{2}$ observed in Ref. 8 is exact.

¹⁰K. Nagasawa, Mater. Res. Bull. **6**, 853 (1971).

¹¹Powder patterns obtained below 125 K in a pure sample of Ti_4O_7 did not show the extra reflections reported in earlier work, Refs. 1 and 3.

¹²R. D. Shannon and C. T. Prewitt, Acta Crystallogr. **B25**, 925 (1969).

¹³A slightly lower value for $V^{4+}-O$ is given which is based on recent refinements of the structures of VO_2 and $\text{VO}_2 + 2.4 \text{ at.}\% \text{ Cr}$.

¹⁴J. B. Goodenough, J. Solid State Chem. **3**, 490 (1971), and Progr. Solid State Chem. **5**, 145 (1971).

¹⁵A. C. Gossard and J. P. Remeika, Bull. Amer. Phys. Soc. **17**, 359 (1972).

Ultrasonic Studies of Antiferromagnetic Resonance in RbMnF_3 near the Néel Temperature

Takehito Jimbo* and C. Elbaum†

Department of Physics, Brown University, Providence, Rhode Island 02912

(Received 13 April 1972)

Peaks found in the attenuation of transverse and longitudinal ultrasonic waves in RbMnF_3 below the Néel temperature are identified as due to antiferromagnetic resonance on the basis of their temperature-frequency relation and magnetic field dependence. The temperature dependence of antiferromagnetic resonance has thus been determined for $0.1^\circ\text{K} \lesssim T_N - T \lesssim 4^\circ\text{K}$, where T_N is the Néel temperature.

The cubic and nearly isotropic antiferromagnet RbMnF_3 has been extensively investigated. In particular, various aspects of ultrasonic propa-

gation,¹⁻⁷ as well as conventional studies of antiferromagnetic resonance (AFMR),^{8,9} have been carried out by a number of workers. As far as